(Received 11 November 2024, Accepted 12 December 2024, Scheduled 30 December 2024)

A Compact Dual Band Wearable Slot Antenna with Partial Ground for WLAN and X Band Applications

Nageswara R. Regulagadda* and Uppalapati V. R. Kumari

University College of Engineering, Jawaharlal Nehru Technological University-Kakinada, Kakinada, A.P., India

ABSTRACT: This study introduces a compact, dual-band wearable slot antenna with inverted L-shaped partial ground (PG) for Wireless Local Area Networks (WLANs) and X-band applications. The proposed antenna design uses a flexible polyamide material of 21×21 mm^2 dimensions as a dielectric substrate between two metal surfaces. The prime radiator is a rectangular slot antenna patch with several slots etched out, and the ground plane is an inverted L-shaped stub that forms the PG. The insertion of slots in the patch disturbs the surface current path and increases the electrical length to offer miniaturizations. It effectively minimizes the antenna dimensions to resonate at lower frequencies. The dimensions of the PG and its placement on the ground plane attain the dual-band resonance with a good amount of return loss. Different slots are etched on the patch to get the desired frequency bands of operation. The designed antenna has achieved wide impedance bandwidths of 0.55 GHz and 1.04 GHz and peak gains of 6.45 dBi and 6.04 dBi at the 5.15 GHz and 8.13 GHz operating frequencies, respectively. The detuning behavior of the suggested antenna in bending conditions is analyzed. The effect of radiation on the human tissue is calculated in terms of Specific Absorption Rate (SAR), and it is within the standards. The antenna model is fabricated and tested, and a satisfactory agreement between the computed and measured data is achieved. The compactness, flexibility, and radiation pattern make this antenna model suitable for ON/OFF-Body communication in wearable applications.

1. INTRODUCTION

Due to wearable devices' ability to have an efficient antenna that can transmit sensed data like vital signs from the human body effectively and quickly, wearables play a crucial part in the current remote health monitoring applications and find themselves in numerous other fields, including wellness & fitness, sports, security, fashion, and other fields. Because antenna is a crucial part of wireless communication and is essential for reliable and effective wireless connectivity, the design of antennas has received the attention from researchers, and several miniaturization techniques have been developed to get the optimum designs for the desired applications. Given that they operate so closely to the human body, wearables should be adaptive to the curvatures of various human body parts, which raises several design difficulties for wearable antennas. Placing an antenna on human flesh can cause the operating frequency to be out of tune because human tissue absorbs electromagnetic energy. The constructed antenna must perform effectively under bending situations and be durable. For the designed antenna to be used for wearable applications, it should also have a low profile, be flexible, be compact, and have a low SAR value.

The proposed work uses a slotted patch with a PG structure to attain dual-band behavior. Slots in the patch can reduce unwanted dispersion of radiation in any particular direction [1]. A few works on the dual-band slot antenna designs from the literature are presented in this section. The authors developed a compact, flexible antenna for Industrial Scientific Medical (ISM) band (902–928 MHz and 2400–2480 MHz) applications [2]. In this design, multiple slots are etched from the radiator to obtain dual-band operation. In [3], the authors achieved the dual-band operation at ISM bands 2.4 GHz and 5.8 GHz by developing a 2×2 Electronic Band Gap (EBG) structure. This EBG structure can act as an Artificial Magnetic Conductor (AMC), and Coplanar Waveguide (CPW) feeding method is used to have resonance with wide bandwidth and gain values at the desired frequency bands.

A semi-flexible wearable antenna that uses meander lines on top of the substrate to excite the higher resonating mode at 5.8 GHz and on the bottom of the substrate to excite the lower resonating mode at 2.45 GHz is presented [4]. For wearable applications, the authors have demonstrated a small textile antenna employing a metasurface [5]. This work involves modifying the dispersion curve of the metasurface unit cell to make the antenna resonate at desired frequency bands. In addition, this work uses a CPW feed with a slot to have a low profile for the planned design. Authors proposed a dual-band multilayer wearable low-profile flexible antenna [6] by altering the behavior of a dipole antenna by inserting meander lines, a rectangular reflector, and parasitic elements into the structure.

The authors in [7] presented a textile antenna built on an AMC that can operate in the 3.5 GHz Worldwide Interoperability for Microwave Access (WiMAX) and 5.8 GHz ISM bands. This design produced high gains of 6.0 dB and 5.8 dB at the operating frequencies. Attaching two homogeneous stubs to the patch and etching a rectangular slot on it attained resonances at two bands, 2.45 GHz and 3.5 GHz [8]. This design offers flexibility, low profile, and high gain. The authors proposed a

* Corresponding author: Nageswara Rao Regulagadda (nageswararao.regula@gmail.com).

TABLE 1. The suggested antenna optimized dimensions.

Parameter	W	$W1$	$W2$	$W3$	$W4$	$W5$	$W6$	L	$L1$
Dimension (mm)	21	19.672	3.11	2.5	15	14.5	1	21	14.31
Parameter	$L2$	$L3$	$L4$	$L5$	$L6$	$L7$	$L8$	$L9$	
Dimension (mm)	1.5	3.5	2.5	6	8	12	2.5	12.5	

TABLE 2. Development stages of the suggested antenna.

Evolution stages	**Frequency (GHz)**	S_{11} **(dB)**	**Bandwidth (GHz)**
Full ground with conventional patch	4.98	-30	1.52
PG with the conventional patch	5.8 & 9.16	-29 & -40	1.27 & 0.38
With slots at the middle of the patch	4.88 & 9.3	-23 & -49	1.32 & 0.52
With slots at the corners of the patch	5.2 & 8.26	-38 & -37	1.44 & 0.55

planar inverted-F antenna (PIFA) and excitation of higher-order modes to resonate at two operating bands for body-centric communications [9]. This structure attained dual-mode operation at the targeted two ISM bands (2.45 GHz and 5.8 GHz).

A work for attaining resonance at two ISM bands for wearable applications is suggested in [10]. This design offers a procedure that results in low SAR values for the entire operating frequency band. The authors developed a ring-like structure that used an inverted L-shaped stub and an F-shaped monopole [11]. Here, out of the two parts of the patch, the upper ring-shaped patch produces lower frequency band, while the lower portion of the F-shaped structure produces higher frequency band. Another novel wearable antenna design backed by an AMC structure is developed for Sub-6 GHz and WLAN applications [12]. This design yields a compact size, directional radiation patterns, and an impedance bandwidth of 31%. From the literature stated above, it is evident that some works are complex in design, a few do not use flexible materials, and some are large. So, this work proposes an antenna design with a small size, flexible substrate, and simple design to address the challenges associated with above mentioned works from the literature.

2. ANTENNA DESIGN

The proposed antenna design uses a flexible polyamide fabric of 1.6 mm thickness as the substrate material. The substrate's dielectric constant ε_r) is 4.3, and the loss tangent ($\tan\delta$) is 0.004. It is a flexible, durable, lightweight synthetic material [13]. Copper material is used for the ground layer and patch layer. The total size of the antenna is 21 mm $\times$ 21 mm. A 50-ohm microstrip feed is used for the excitation of the proposed design. Here, the patch has dimensions of 19.672 mm $\times$ 14.5 mm. The proposed antenna uses High Frequency Structure Simulator (HFSS) tool for the antenna design and the method of chemical vapor decomposition in the fabrication process.

The design of the suggested antenna first considers a rectangular plain patch with a complete ground plane. Single-band resonance then results from the reduction of the entire ground plane to an I-shaped PG. The dual-band resonance is achieved by adding one more I-shaped stub at its end at a 90-degree angle in the positive X-direction, creating an inverted L-shaped ground plane. There are two kinds of slots in the radiating patch. Out of the two, one set has four square-shaped slots at the patch's four corners, and the other set has an array of slots arranged in the middle of the patch like a Yagi-Uda antenna. The slots on the patch resulted in shifting the frequency bands towards lower frequencies, improving the return loss for both frequency bands and obtaining the resonance at the targeted frequency of operation, 5.15 GHz and 8.13 GHz.

Figure 1 depicts the design model of the suggested antenna. Figures 1(a) and 1(b) show the antenna design by using the HFSS tool, Figures 1(c) and 1(e) depict the top view; Figure 1(d) shows the bottom view of the fabricated antenna; and Figure 1(f) explores the antenna arrangement in the anechoic chamber. Table 1 shows the optimized dimensions of the proposed antenna design.

3. PARAMETRIC ANALYSIS

Initially, a rectangular patch with the entire ground plane is considered in the design of the suggested antenna, able to resonate at different frequencies with very high return loss and very narrow bandwidths. Then, the complete ground plane is modified to a PG in the first stage with a length of 2.5 mm, achieving resonance at 4.98 GHz with wide bandwidth and at another frequency beyond 10 GHz with narrow bandwidth. In the second stage, the PG is modified to get dual resonant frequencies and can get resonance at 5.81 GHz and 9.16 GHz. When a series of rectangular slots are arranged like a Yagi-Uda antenna at the center of the patch, the antenna then displays resonance at 4.91 GHz and 9.3 GHz. Finally, the antenna achieved resonance at the two desired bands of 5.2 GHz and 8.26 GHz by placing square slots close to the patch's four corners. Figures 2(a) and 2(b) show the various stages of antenna development and the return loss graph for each stage of antenna development. Table 2 lists the specifics of antenna parameters.

Figure 3 deals with the return loss graph for various ground dimensions of the proposed antenna. Figures 3(a)–3(d) display the S_{11} graph for different W6, L9, W5, and L8 values.

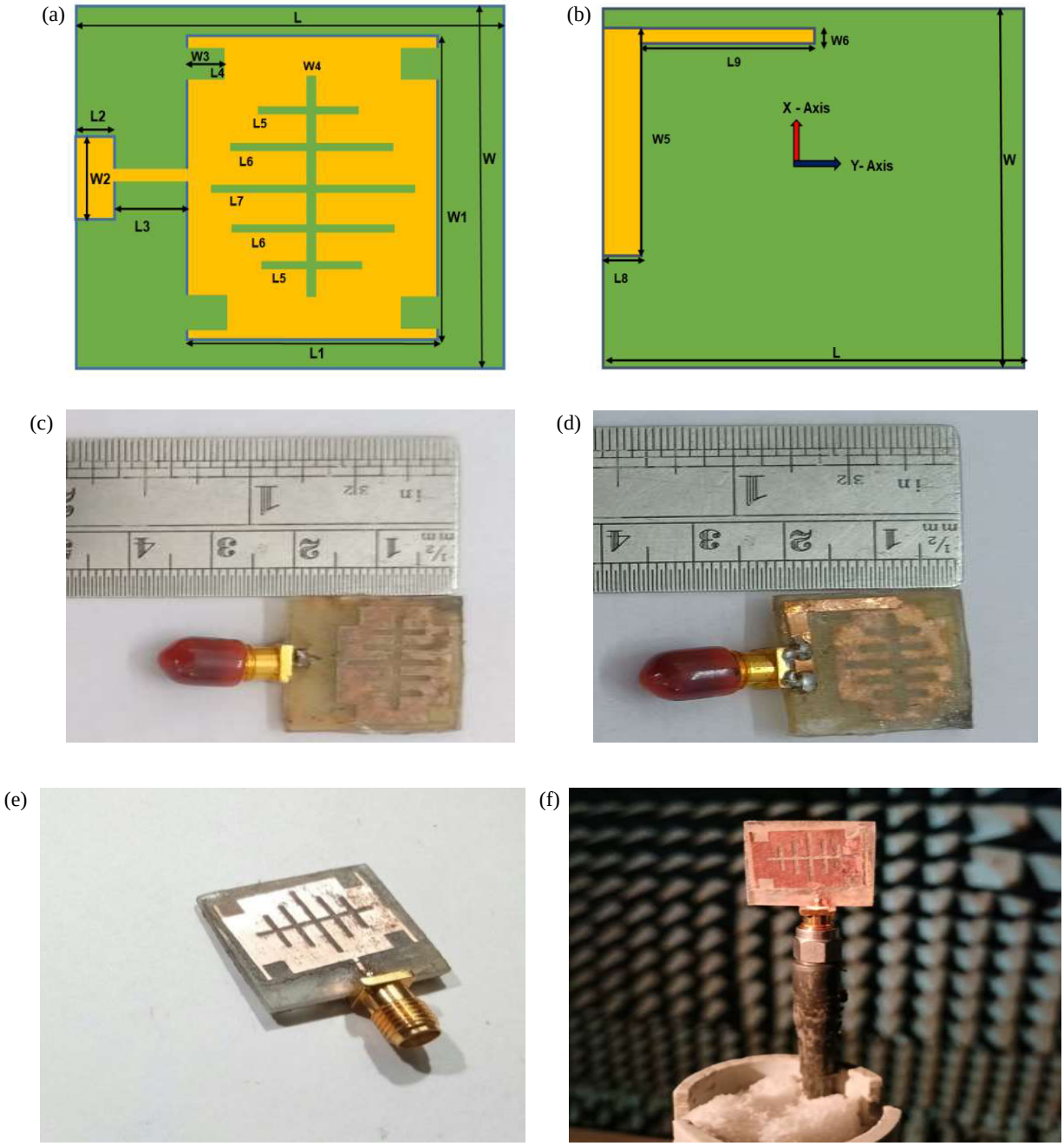

FIGURE 1. Antenna design models. (a) Simulated_top-view. (b) Simulated_bottom-view. (c) Prototype_top-view. (d) Prototype _bottom-view. (e) Fabricated antenna. (f) Antenna in anechoic chamber.

With an increase in the value of W6, the resonating frequencies shift towards higher frequencies with high losses. The decrease in L9 value leads to the shifting of resonating frequency towards lower frequencies with higher losses, and an increase in its value deviates from desired resonating frequencies and the multiband behavior also at L9 of 16 mm. Figure 3(c) shows that there is not much change in the S_{11} graph with different dimensions for W5 (mm). Figure 3(d) explains that with a decrease in the value of L8, the resonating frequencies shifted toward the higher frequencies and resulted in high loss. The increase in its value resulted only in return losses. With a change in W5, W6, L8, and L9, the S_{11} (dB) value changes significantly while the gain and radiation patterns look the same.

4. RESULTS AND DISCUSSIONS

This section presents the computed results, measured results, and details about the comparison results of the suggested antenna. Adjusting the slots on the patch and varying their dimensions, placing them at different positions resulted in the antenna resonance at two frequencies, 5.2 GHz and 8.26 GHz, with an impedance bandwidth of 1.44 GHz and 0.52 GHz, re-

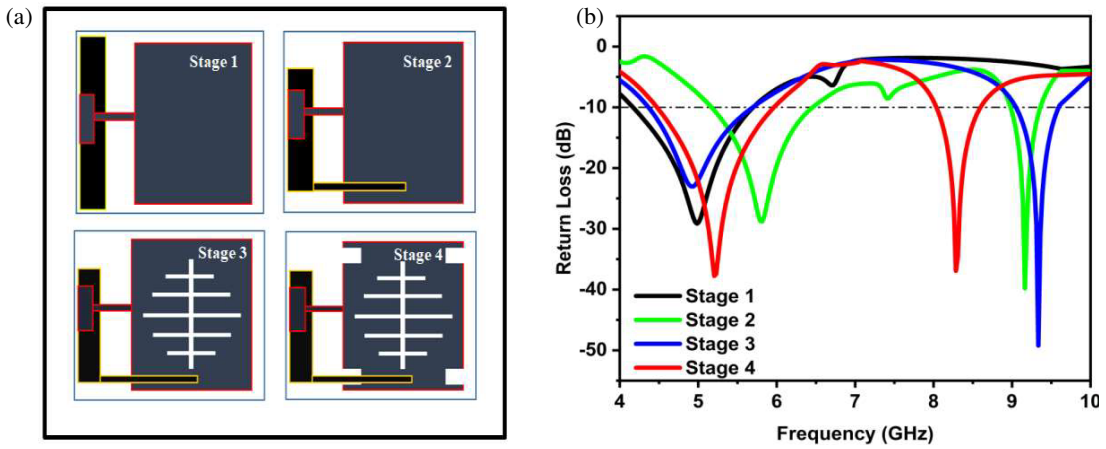

FIGURE 2. (a) Antenna development stages. (b) S_{11} graph for different stages of antenna development.

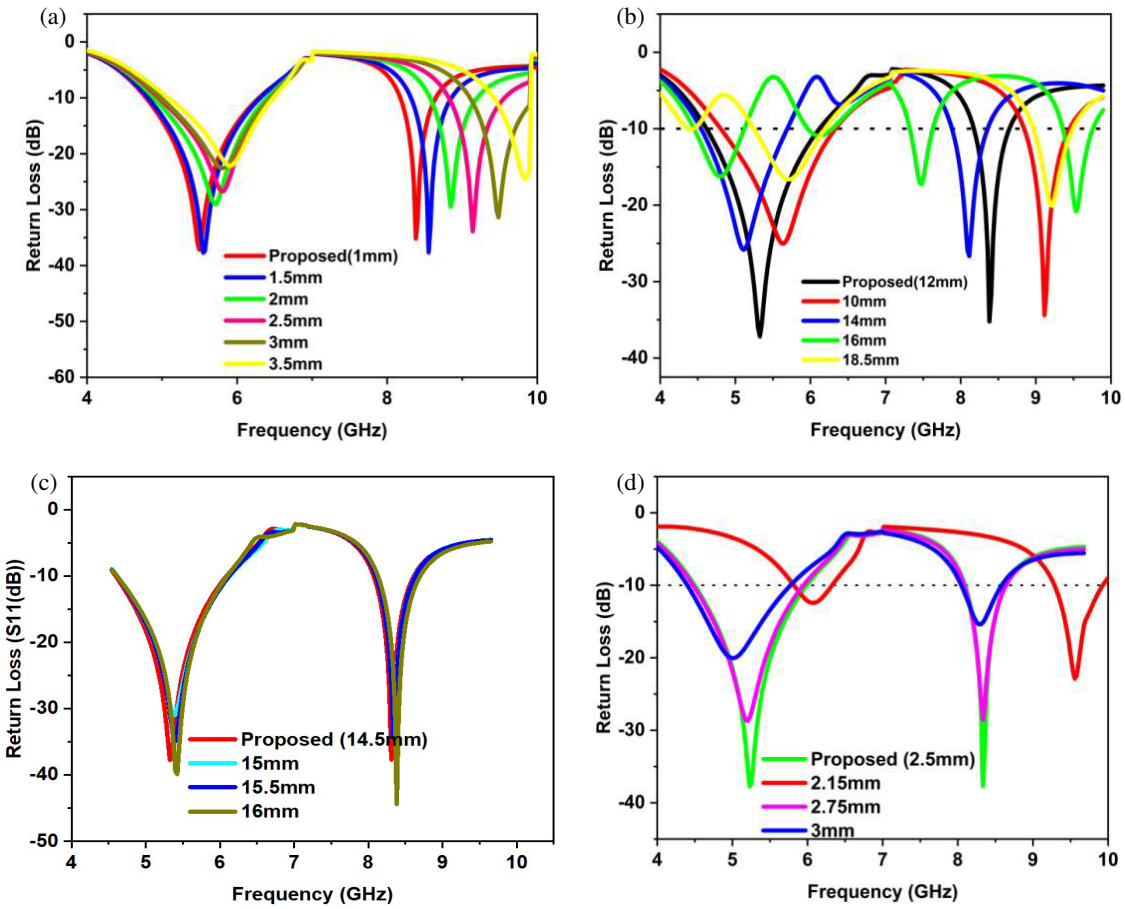

FIGURE 3. Parametric analysis — Return loss graph for various values of (a) W6, (b) L9, (c) W5, (d) L8.

spectively. The designed antenna achieved the simulated directive gains of 6.8 dB and 7.4 dB throughout the two operating frequency bands. Figure 4 represents the simulated results of the proposed antenna. Figure 4(a) shows the co-polarization and cross-polarization plot at 5.2 GHz; Figure 4(b) explores the co-polarization and cross-polarization plot at 8.2 GHz; Figure 4(c) depicts the electric field plot at 5.2 GHz; and Figure 4(d) represents the electric field plot at 8.2 GHz.

4.1. Measured Results

The proposed antenna is fabricated using the vapor decomposition method and tested using Agilent N5247A: A.09.90.02 network analyzer. Figure 5 shows the measured return loss graph in different scenarios, and Figure 6 depicts the comparison results of the measured and computed parameters of the proposed antenna. Figure 5(a) shows the return Loss graph in free space; Figure 5(b) represents it on a human arm; and Fig-

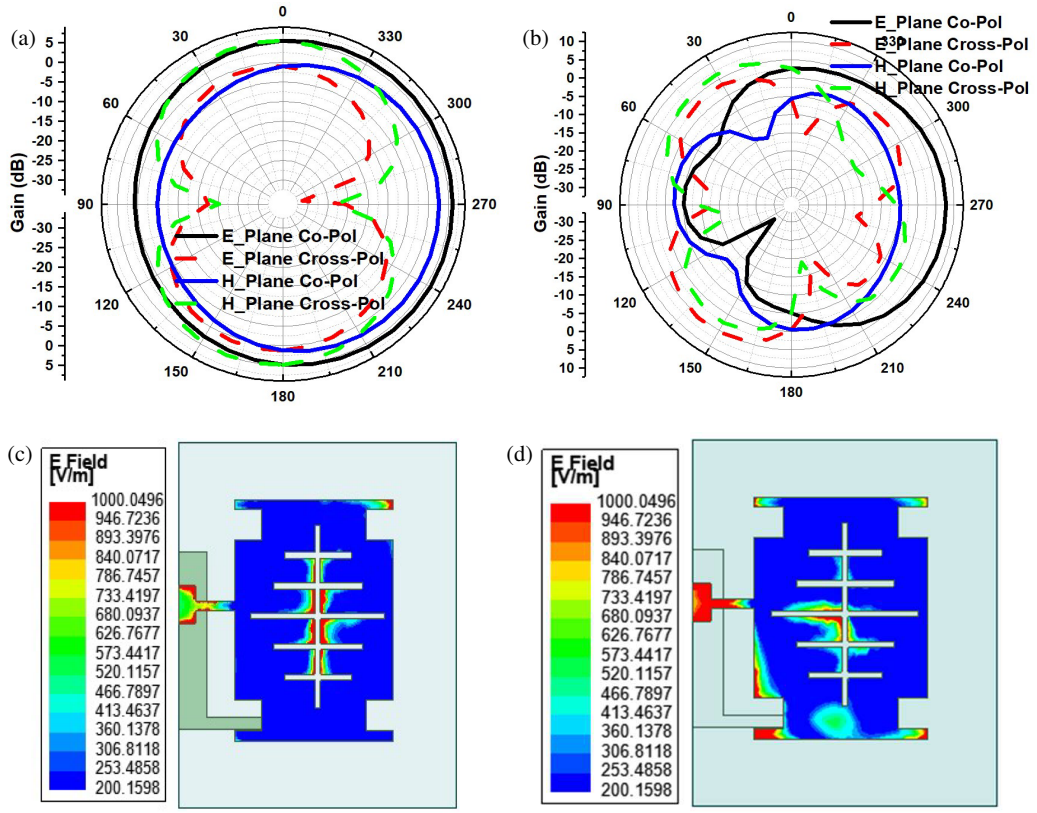

FIGURE 4. Simulation results of proposed antenna. (a) Co-Pol & Cross-Pol radiation pattern at 5.2 GHz. (b) Co-Pol & Cross-Pol radiation pattern at 8.26 GHz. (c) Electric field plot at 5.2 GHz. (d) Electric field plot at 8.2 GHz.

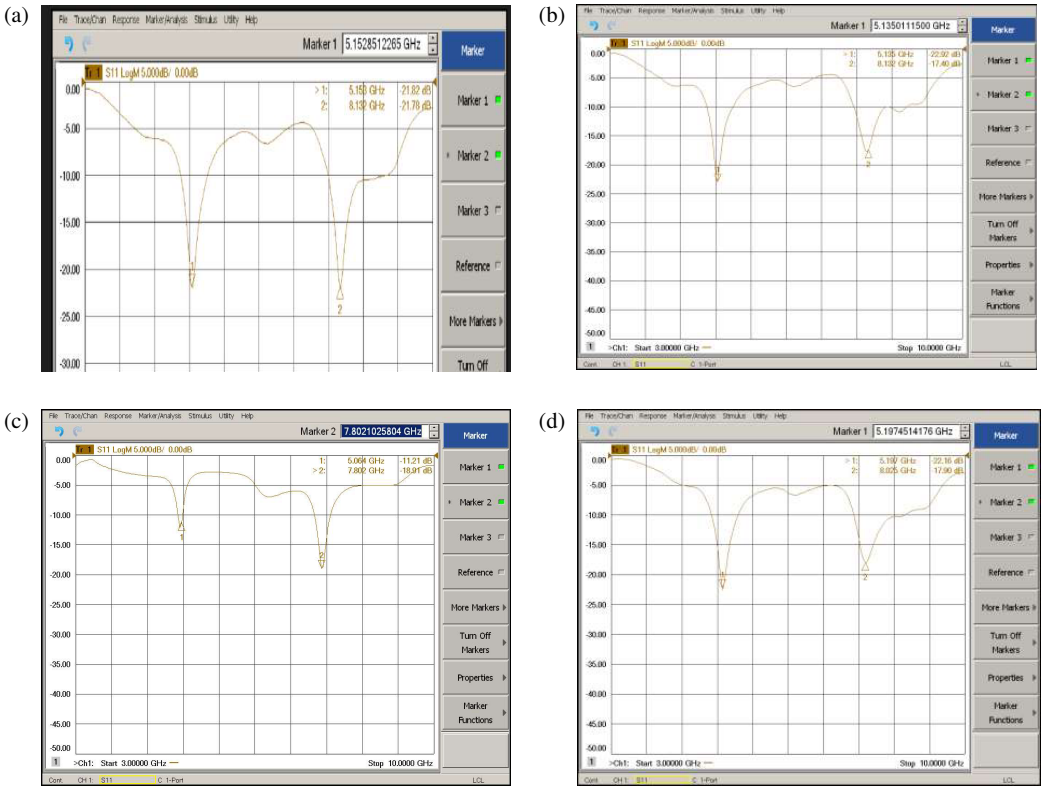

FIGURE 5. Antenna measured results — Return Loss. (a) Free space. (b) On human Arm. (c) Bend in X-axis. (d) Bend in y-axis.

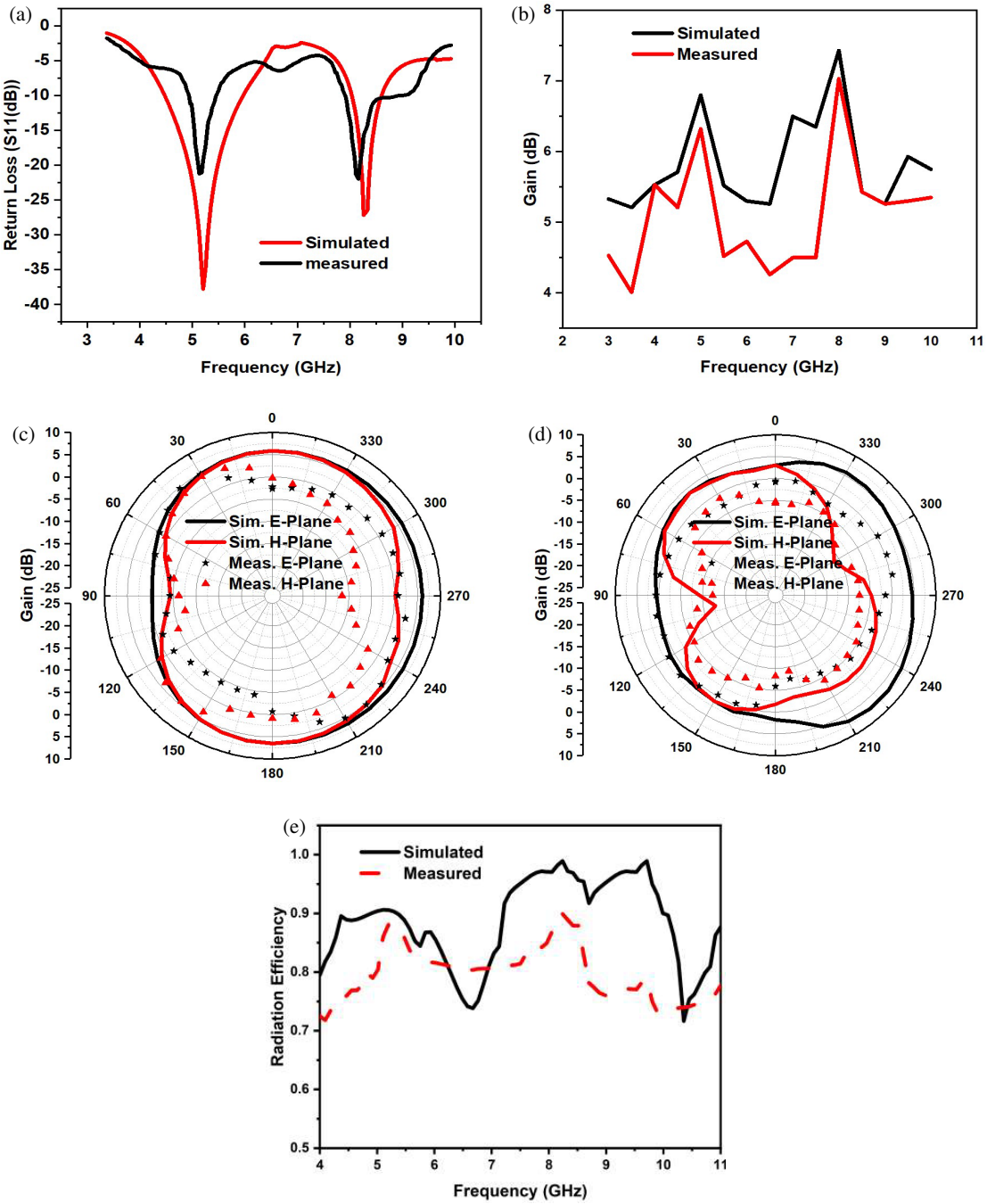

FIGURE 6. Results comparison. (a) Return loss, S_{11} (dB). (b) Gain. (c) Radiation pattern at 5.15 GHz. (d) Radiation pattern at 8.13 GHz. (e) Radiation efficiency.

ures 5(c) and 5(d) explore it when the antenna is bent in X-axis and y-axis, respectively. From Figure 5(a), it is clear that the fabricated antenna resonates at 5.153 GHz and 8.132 GHz with an impedance width of 550 MHz (4.9 GHz–5.45 GHz) and 1040 MHz (7.89 GHz–8.93 GHz), respectively. The fractional bandwidths at the mid-frequency of the resonating frequencies are 10.6% and 12.36%, and the gains are 6.4 dBi and 6.04 dBi, respectively. Figures 6(a)–6(e) show the comparison graphs of both computed and measured results.

4.2. Test of Wearability

The designed antenna is analyzed for its validity to wearable applications in terms of unchanged characteristics in the presence of human tissue in bent and unbent conditions. The human loading effect on the antenna parameters and the SAR value of the antenna are also analyzed. The following sections furnish the details of this analysis.

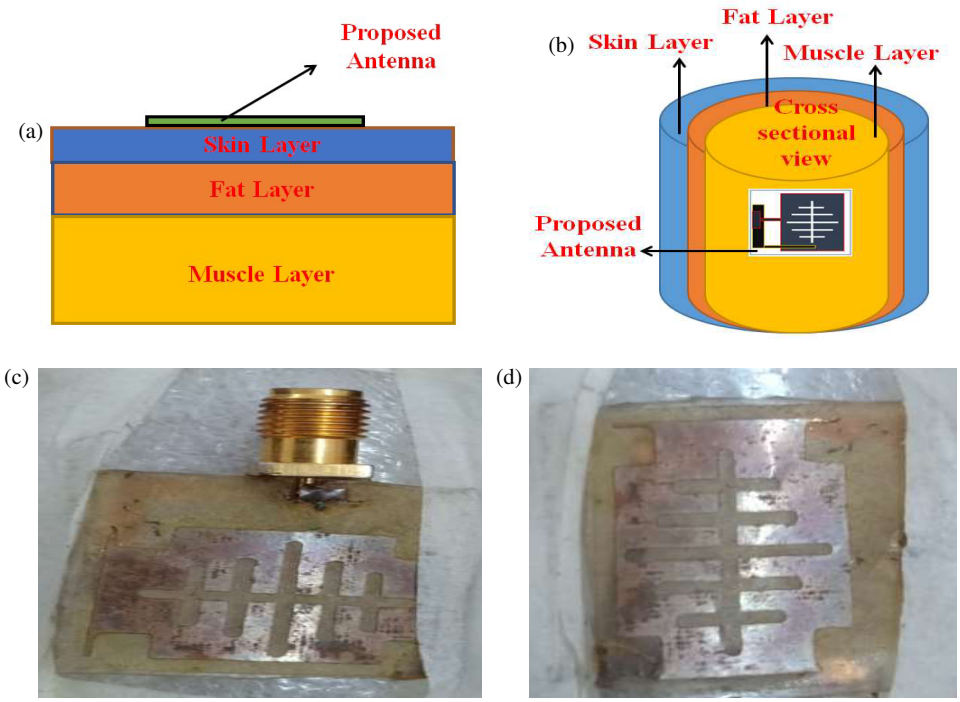

FIGURE 7. Antenna's human loading setup. (a) Placed on flat human surface. (b) Placed on bent human surface. (c) Bent in X-Axis. (d) Bent in Y-Axis.

TABLE 3. The proposed work's comparison with the literature.

Reference	Antenna Dimensions (mm^2)	Method of miniaturization	Operating Frequency (GHz)	Fractional Bandwidth (%)	Gain (dBi)
[4] 2020	19×12	Meander with strips	2.45, 5.8	5.7, 3.78	2.1, 3.5
[5] 2022	44.1×44.1	Metasurface	2.45, 5.5	10.2, 22.5	-0.67, 7.4
[6] 2018	50×40	Meandered lines	2.47, 5.42	20, 19	1.17, 1.17
[7] 2021	62×62	AMC	3.5, 5.8	12.5, 11.6	6, 5.8
[11] 2022	41×44	Slots	2.4, 5.8	3.75, 5.17	3.74, 5.13
[12] 2023	38×38	AMC	5.2	31	5
This work	**21×21**	**Slots with PG**	**5.15, 8.13**	**10.6, 12.36**	**6.45, 6.04**

4.2.1. Bending Analysis

The dependency of various antenna parameters of the designed antenna is examined by keeping it on flat and curved human tissues. This feature is vital in ON/OFF communication environments. The antenna must be adaptable to accommodate the varying forms of various human tissues. Figure 7(a) shows the arrangement of human loading, and 7(b) presents the placement of the suggested antenna on a curved three-layer human tissue model. Figures 7(c) & 7(d) show the antenna bent in X-axis and Y-axis, respectively.

4.2.2. Human Loading

To study the effect of human loading on the antenna parameters values, a three-layer human tissue model with skin, fat, and muscle layers is designed [13] using an HFSS EM simulator tool. At 2.4 GHz and 5.8 GHz frequencies, the electrical properties of skin, fat, and muscle tissues are mentioned [14]. Figure 7 shows the human tissue model setup. The suggested antenna has a three-layer human tissue structure, with the top layer being skin, the middle layer being fat, and the bottom layer being muscle. Figure 8 highlights the outcomes like S_{11} (Figure 8(a)), gain (Figure 8(b)), and radiation characteristics (Figure 8(c) and 8(d)) of the proposed antenna when the proposed antenna is attached to the human tissue. The proposed antenna's performance when it is bent and when it is loaded with human tissue is compared with the unbent and freespace performance, and it is found that there is no much deviation in its performance in both the cases. Thus, the antenna attains stable performance in these two scenarios. Figure 8(e) shows the arrangement of the fabricated antenna on a human hand.

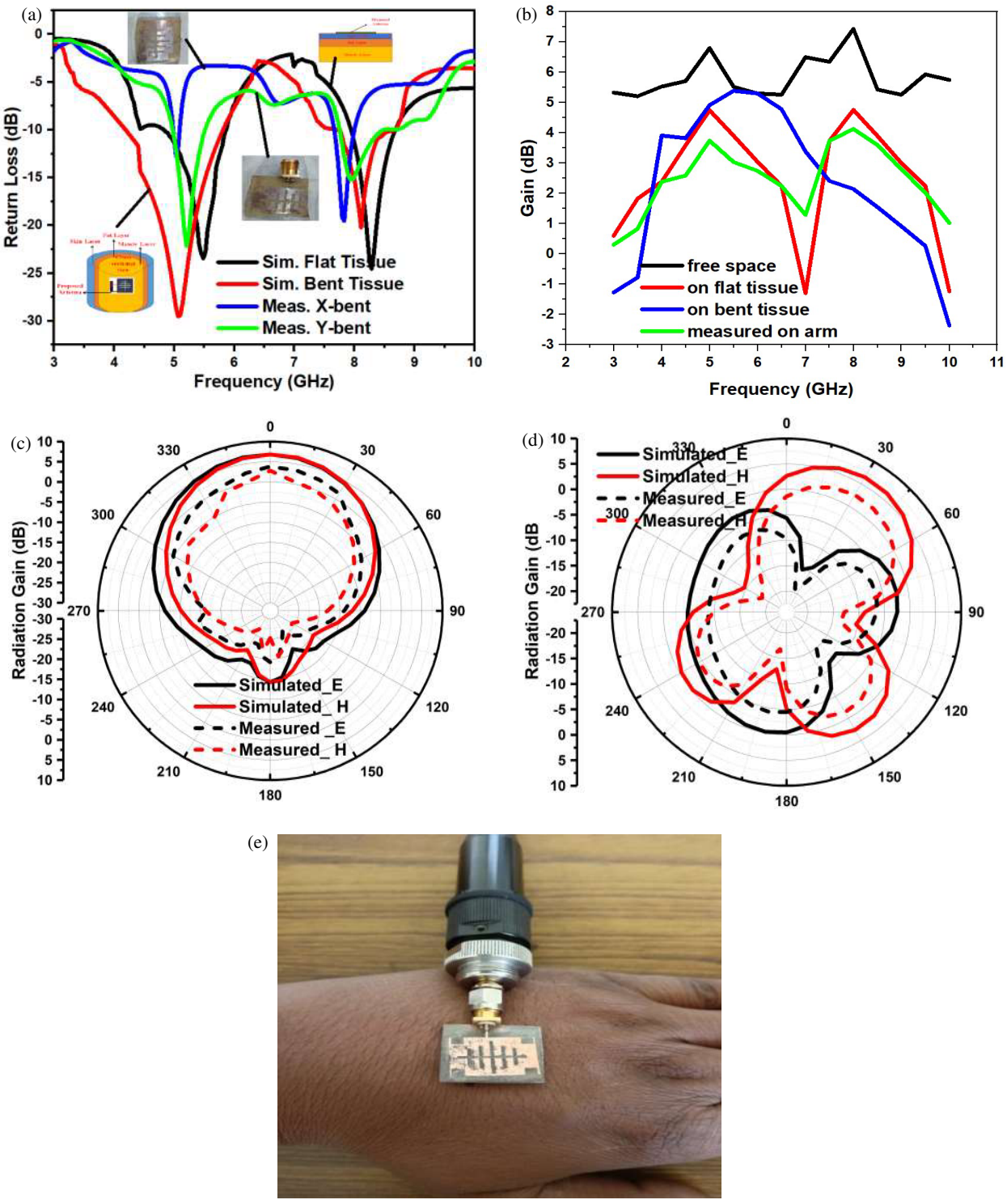

FIGURE 8. Wearability test. (a) S_{11} comparison. (b) Gain comparison. (c) Radiation pattern comparison @ 5.2 GHz. (d) Radiation pattern comparison at 8.26 GHz. (e) Fabricated antenna on human hand.

4.2.3. SAR Calculation

The SAR is a unit of measurement for the quantity of electromagnetic energy that human tissue absorbs, and it is necessary to evaluate the SAR as it deals with human wellness, especially in wearable scenarios. The proposed antenna must not exceed the SAR limits of US/EU standards. The average SAR is carried out for both operating frequencies by placing the proposed antenna on the three-layer human tissue model. It is found from Figure 9 that the SAR value is far below the standards when being averaged over 1 gm of human tissue for an input power of less than 0.5 Watts. If the SAR value is not below the criteria,

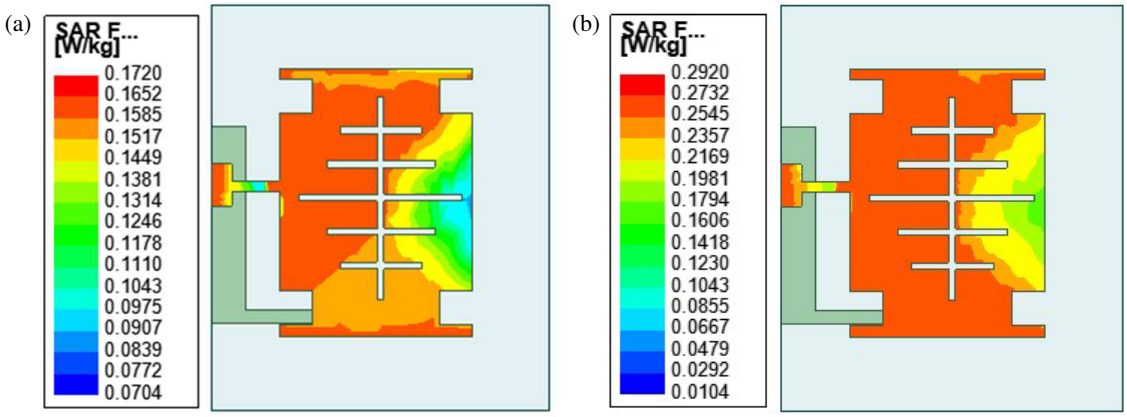

FIGURE 9. SAR analysis. (a) SAR @ 5.2 GHz. (b) SAR @ 8.2 GHz.

alternative ways are suggested in the literature [15, 16]. Figures 9(a) and 9(b) depict the simulated average SAR at 5.2 GHz and 8.2 GHz, respectively. Table 3 explores the comparison of the antenna parameters of the proposed work with the literature.

5. CONCLUSIONS

This work introduces a dual-band compact, flexible, and wideband slot antenna for wearable applications. A flexible polyamide substrate is used in the antenna design with a compact size of $21 \times 21\,\text{mm}^2$ to make it suitable for wearable applications. Placing different slots at different positions on the patch resulted in antenna resonance at dual frequencies of 5.15 GHz (WLAN) and 8.13 GHz (X-band). The results show that the designed antenna has attained good return loss values and wide bandwidth with a good gain for two frequency bands. The flexibility or conformability of the designed antenna is checked for wearable applications and obtained justified results. The designed antenna is fabricated and obtains measured results. The results from computation and fabrication are in good accord. The proposed work's attractive radiation pattern, compact size, and the use of a flexible substrate make this a good candidate for On/Off-Body communication applications. This proposed work can be modified to achieve multiband functionality, allowing a single antenna to cater to a broader range of applications while ensuring excellent isolation between bands. Additionally, incorporating reconfigurability in the cases of pattern, polarization, or frequency can further enhance the antenna's versatility and performance across various use cases.

REFERENCES

[1] Li, H., J. Du, X.-X. Yang, and S. Gao, "Low-profile all-textile multiband microstrip circular patch antenna for WBAN applications," *IEEE Antennas and Wireless Propagation Letters*, Vol. 21, No. 4, 779–783, Apr. 2022.

[2] Singh, H., K. Srivastava, S. Kumar, and B. K. Kanaujia, "A planar dual-band antenna for ISM/Wearable applications," *Wireless Personal Communications*, Vol. 118, 631–646, 2021.

[3] Dalal, P., U. Rafique, S. M. Abbas, N. C. Pradhan, and S. S. Karthikeyan, "Dual-band wearable antenna for wireless body area networks on a flexible substrate," in *2022 IEEE Wireless Antenna and Microwave Symposium (WAMS)*, 1–5, Rourkela, India, 2022.

[4] Le, T. T. and T.-Y. Yun, "Miniaturization of a dual-band wearable antenna for WBAN applications," *IEEE Antennas and Wireless Propagation Letters*, Vol. 19, No. 8, 1452–1456, Aug. 2020.

[5] Zhang, K., P. J. Soh, and S. Yan, "Design of a compact dual-band textile antenna based on metasurface," *IEEE Transactions on Biomedical Circuits and Systems*, Vol. 16, No. 2, 211–221, Apr. 2022.

[6] Al-Sehemi, A., A. Al-Ghamdi, N. Dishovsky, N. Atanasov, and G. Atanasova, "Design and performance analysis of dual-band wearable compact low-profile antenna for body-centric wireless communications," *International Journal of Microwave and Wireless Technologies*, Vol. 10, No. 10, 1175–1185, 2018.

[7] Yang, H. and X. Liu, "Screen-printed dual-band and dual-circularly polarized textile antenna for wearable applications," in *2021 15th European Conference on Antennas and Propagation (EuCAP)*, 1–4, Dusseldorf, Germany, 2021.

[8] Chuquitarco-Jiménez, C. A., E. Antonino-Daviu, and M. Ferrando-Bataller, "Dual-band antenna with AMC for wearable applications," in *2021 15th European Conference on Antennas and Propagation (EuCAP)*, 1–4, Dusseldorf, Germany, 2021.

[9] Dang, Q. H., S. J. Chen, B. Zhu, and C. Fumeaux, "Dual-band dual-mode wearable textile antennas for on-body and off-body communications," in *2021 IEEE Asia-Pacific Microwave Conference (APMC)*, 64–66, Brisbane, Australia, 2021.

[10] Ahmad, S. and M. A. Shahzad, "A compact size ISM band wearable flexible antenna for IoT smart watch applications," in *2021 1st International Conference on Microwave, Antennas & Circuits (ICMAC)*, 1–4, Islamabad, Pakistan, 2021.

[11] Sharma, R. and S. Kumar, "Compact dual-band wearable antenna for on/off body wireless communication applications," in *2022 IEEE Silchar Subsection Conference (SILCON)*, 1–6, Silchar, India, 2022.

[12] Kulkarni, J., B. Garner, and Y. Li, "AMC-backed wearable monopole antenna for sub-6 GHz 5G and WLAN applications," in *2023 IEEE International Symposium on Antennas and Propagation and USNC-URSI Radio Science Meeting (USNC-URSI)*, 1265–1266, Portland, OR, USA, 2023.

[13] Regulagadda, N. R. and U. V. R. Kumari, "A low profile wearable slot antenna with partial ground for 5 GHz WLAN/WBAN applications," *Progress In Electromagnetics Research C*, Vol. 128, 183–193, 2023.

[14] Ali, U., S. Ullah, B. Kamal, L. Matekovits, and A. Altaf, "Design, analysis and applications of wearable antennas: A review," *IEEE Access*, Vol. 11, 14 458–14 486, 2023.

[15] Zebiri, C., D. Sayad, I. Elfergani, A. Iqbal, W. F. A. Mshwat, J. Kosha, J. Rodriguez, and R. Abd-Alhameed, "A compact semi-circular and arc-shaped slot antenna for heterogeneous RF front-ends," *Electronics*, Vol. 8, No. 10, 1123, 2019.

[16] Augustine, R., T. Alves, T. Sarrebourse, B. Poussot, K. T. Mathew, and J.-M. Laheurte, "Polymeric ferrite sheets for SAR reduction of wearable antennas," *Electronics Letters*, Vol. 46, No. 3, 197–198, 2010.